ELSEVIER

Computer-Aided Design 37 (2005) 1127–1139

COMPUTER-AIDED DESIGN

www.elsevier.com/locate/cad

Bayesian computer-aided experimental design of heterogeneous scaffolds for tissue engineering

L.E. Weiss*, C.H. Amon, S. Finger, E.D. Miller, D. Romero, I. Verdinelli, L.M. Walker, P.G. Campbell

Carnegie Mellon University, Pittsburgh, PA, USA

Accepted 2 February 2005

Abstract

This paper presents a Bayesian methodology for computer-aided experimental design of heterogeneous scaffolds for tissue engineering applications. These heterogeneous scaffolds have spatial distributions of growth factors designed to induce and direct the growth of new tissue as the scaffolds degrade. While early scaffold designs have been essentially homogenous, new solid freeform fabrication (SFF) processes enable the fabrication of more complex, biologically inspired heterogeneous designs with controlled spatial distributions of growth factors and scaffold microstructures. SFF processes dramatically expand the number of design possibilities and significantly increase the experimental burden placed on tissue engineers in terms of time and cost. Therefore, we use a multi-stage Bayesian surrogate modeling methodology (MBSM) to build surrogate models that describe the relationship between the design parameters and the therapeutic response. This methodology is well suited for the early stages of the design process because we do not have accurate models of tissue growth, yet the success of our design depends on understanding the effect of the spatial distribution of growth factors on tissue growth. The MBSM process can guide experimental design more efficiently than traditional factorial methods. Using a simulated computer model of bone tissue regeneration, we demonstrate the advantages of Bayesian versus factorial methods for designing heterogeneous fibrin scaffolds with spatial distributions of growth factors enabled by a new SFF process.

Keywords: Tissue engineering; Solid freeform fabrication; Heterogeneous designs; Bayesian modeling

1. Introduction

Our goal is to create tissue engineered therapies to treat hard-to-heal wound sites by designing and manufacturing implantable scaffolds with growth factors that recruit cells from the host's surrounding healthy tissue into the scaffolds, and then guide new tissue growth as the scaffolds are degraded by these invading cells. Fig. 1 shows a candidate therapy for use in a calvarial (skull) critical sized defect (CSD), i.e. a defect that is too large for the bone to regenerate spontaneously unless treated with a bone promoting therapy [1]. Calvarial defects are often chosen for testing bone repair materials because the skull has a poor blood supply and a deficiency of bone marrow, making a demanding test for a candidate therapy [2]. The design in Fig. 1, which will be used as an example throughout this paper, consists of spatial patterning of two growth factors, fibroblast growth factor-2 (FGF-2) and bone morphogenetic protein-2 (BMP-2), delivered in a bi-density fibrin scaffold. The dense and less dense regions are interconnected in a cross-hatch architecture. To design and fabricate such an implant successfully requires:

- a manufacturing process capable of fabricating heterogeneous structures with complex architectures, and
- an understanding of the relationship between the spatial patterning of growth factors and the resulting bone regeneration in order to optimize the design parameters.

In this paper, we describe a solid freeform fabrication (SFF) process we are developing which can manufacture heterogeneous fibrin-based scaffolds. This process dramatically expands the space of possible designs and parameter combinations, because both the microstructure of

* Corresponding author. Tel.: +1 412 268 7657.
E-mail address: lew@cs.cmu.edu (L.E. Weiss).

0010-4485//$ - see front matter © 2005 Elsevier Ltd. All rights reserved.
doi:10.1016/j.cad.2005.02.004

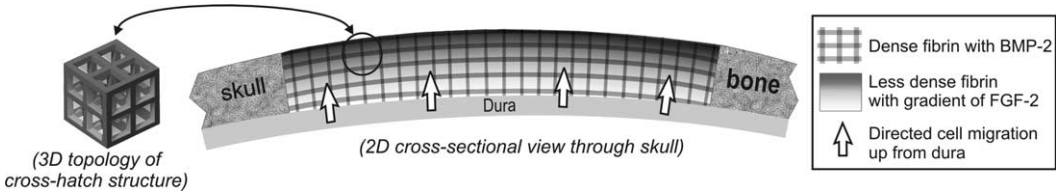

Fig. 1. Example of a candidate heterogeneous scaffold design with a spatial patterning of two growth factors, FGF-2 and BMP-2, and two densities of fibrin.

the scaffold and the distribution of growth factors, within the scaffold, can be controlled precisely. For example, consider a conventional factorial experimental design using the following parameters and values in an in vivo study to determine the therapy effectiveness and optimal values of the parameters:

- four values of FGF-2 concentration gradient magnitude: [$0_{control}$, $Low_{FGF\text{-}2}$, $Med_{FGF\text{-}2}$, $Hi_{FGF\text{-}2}$]
- four values of BMP-2 concentration: [$0_{control}$, $Low_{BMP\text{-}2}$, $Med_{BMP\text{-}2}$, $Hi_{BMP\text{-}2}$]
- three values of fibrin density in dense region: [Low_{fibrin}, Med_{fibrin}, Hi_{fibrin}]

Using a traditional factorial design approach, this would result in 48 ($4\times4\times3$) combinations of treatment options. Using a rabbit in vivo model, observing bone regeneration at three separate time endpoints (e.g. sacrificing rabbits at 4, 8 and 12 weeks post-surgery), using eight rabbits per treatment group for each time endpoint for a total of 1152 rabbits, and processing a maximum of 60 rabbits per year results in a conservative estimate of $873,000 in costs over a 19 year timeframe. This estimate demonstrates that a conventional factorial design approach is not practical. One option would be to first use faster less expensive in vitro studies to pre-screen the designs and narrow the number to the best performers for subsequent in vivo testing. However, in vitro results do not necessarily correlate well with in vivo responses. Ultimately, the tissue engineer would have to use past experience, insight, and intuition to make decisions to limit the number of in vivo tests. However, this ad hoc approach could produce sub-optimal designs and limit gaining further insight about the interactions of the scaffold components and their contributions to healing.

The large number of design possibilities and the combinatorial explosion that results from using standard factorial design underscores the need for more efficient ways to search the parameter space of design possibilities. To address this challenge, we describe a Multi-stage Bayesian Surrogate Modeling (MBSM) methodology that can be used to construct computational models that guide experimental design by quantifying the interactions among variables and performance outcomes. In combination, SFF and MBSM will make possible the design and fabrication of heterogeneous scaffolds for bone tissue engineering.

1.1. Solid freeform fabrication (SFF)

SFF refers to computer-aided-design/computer-aided-manufacturing (CAD/CAM) methods that can fabricate complex shapes automatically from CAD models [3]. SFF processes are based on a layered manufacturing paradigm that builds shapes by incremental material deposition and fusion of thin cross-sectional layers. Decomposing complex 3D shapes into simpler 2D layers dramatically simplifies computer-assisted planning and fabrication of parts. SFF processes also provide full access to the interior of parts as they are being built. Therefore, shapes with complex interior architectures can be fabricated, enabling scaffolds with controlled microstructures to be built for tissue engineering applications [4–17]. In addition to the capability of manufacturing scaffolds with custom shapes and complex internal architectures, it will be important for next-generation scaffold designs to include heterogeneous compositions incorporating controlled spatial distributions of cells, growth factors, and material compositions in order to better mimic aspects of nature or to enable biologically inspired engineered designs. In general terms, SFF methodology enables heterogeneous designs through the use of selective material deposition processes and by simultaneous embedding of discrete components during deposition [17–19]. For tissue engineering applications, we proposed the extension of SFF methodology to build heterogeneous scaffold designs by selectively adding cells and growth factors to the layers as the scaffolds are being built [20]. Numerous investigators have since demonstrated SFF can control the 3D spatial distributions of the biological factors throughout these structures [7,21–30].

Effective use of SFF to build scaffolds requires CAD tools for modeling, informatics, structural analysis, and process planning. Numerous investigators are addressing these needs; Sun et al. [31,32] provide an excellent review of such computer-aided tissue engineering techniques. However, an often-overlooked design issue is that SFF enables the space of design possibilities to expand dramatically. Now, tissue engineers can consider the incorporation of multiple factors and material compositions in a continuum of spatial arrangements throughout the scaffold, resulting in a combinatorial explosion of design possibilities. The biological experimentation required to test and optimize the parameters of any new design, especially in vivo, is typically time consuming and expensive, so tissue

engineers are limited in the number of experimental trials that they can conduct. While the existing large bodies of biological and clinical knowledge can help to inspire new designs and guide parameter selections, this knowledge-base is not mature enough to provide models of wound healing that can serve as a basis for designing heterogeneous matrices.

1.2. Multi-stage Bayesian surrogate modeling (MBSM)

In some design domains, particularly in rapidly evolving domains such as tissue engineering, analytical representations of system behaviors do not exist. In such domains, the design process can be facilitated by the development of surrogate models that provide an understanding of the interactions of parameters and their influence on system performance, even though the models do not explain the underlying phenomena. Many different techniques can be used to build surrogate models, including neural networks, radial basis functions, response surface methodologies, and kriging. Surrogate models can reduce the number of experiments needed and increase the value of the information gained through experimentation. A detailed explanation and comparison of these methods can be found in Jin et al. [33] and Simpson et al. [34]. The main points of comparison are as follows. Response surface is the most widely used method due to its simplicity. Its accuracy depends on the complexity of the response to be modeled. It assumes random errors and does not behave well for highly non-linear responses. Neural networks are better suited for highly non-linear responses and for problems with a large number of parameters. Due to the computational expense of training the network, it is best suited for applications that repeat evaluations. Radial basis functions are easy to apply given the simplicity of the interpolation method. This technique is usually dependable and generates good surfaces in most situations. Kriging is flexible and well suited for deterministic applications. Due to the complexity of the method, applications usually entail fewer than 50 parameters.

We have developed a MBSM methodology, based on a kriging approach, for design and optimization of complex systems and have successfully applied it to several non-biological processes [35–38]. We follow a statistical Bayesian approach in which probability is regarded as a degree of belief. Within the Bayesian framework, a prior distribution is specified to represent what is known (degree of belief) about the process before data is available. As data is collected, the prior distribution is updated to obtain the posterior distribution. Bayesian analysis offers a mathematically rigorous framework in which information is updated based on previous outcomes [39]. In this methodology, we select particular combinations of input parameters, perform experiments at the selected points in the design space, and then construct surrogate computational models that quantify the interactions among variables and predict performance outcomes. At each stage, the current model serves as the prior expectation for the next set of experiments, enabling us to maximize the information gained from each experimental trial [35]. Thus, multi-stage Bayesian modeling can reduce the number of experiments and shorten the timeline for iterative design testing.

2. Heterogeneous fibrin scaffold

2.1. Rationale for the scaffold design

Fibrin was selected as the scaffold material for the candidate therapy in Fig. 1 for several reasons. Fibrin is a native hydrogel that, upon injury, forms a clot in the wound site to stop bleeding, and then it acts as a temporary extracellular matrix for supporting the subsequent cascade of wound healing events [40]. These events include invasion of host cells from the healthy surrounding tissue into the fibrin extracellular matrix, followed by the making of new bone tissue by these cells as the fibrin extracellular matrix degrades. Fibrin degradation is controlled by cell-directed proteolysis (i.e. the invading cells digest the fibrin), with the degradation rate controlled by the resident cells involved in the tissue regeneration process [41,42]. The degradation rate thus controls cell access to fibrin-bound growth factors [41]. Our therapeutic target window for the stimulation of bone regeneration in vivo, which is the example discussed in this paper, falls within the first two weeks of scaffold implantation, during which time growth factor stimulation of initial bone regeneration is expected to occur [43–45]. This will enable FGF-2 and BMP-2, which both naturally bind to fibrin, to remain immobilized until fibrin degradation by invading wound healing cells.

In general, the density of a fibrin scaffold affects both its mechanical and biological properties, which in turn influences many key regeneration factors including cell growth, cell spreading, scaffold degradation rate, surgical handling, and stiffness required to initially maintain the scaffold shape in vivo [46]. However, no single density value of a fibrin scaffold can simultaneously optimize all these factors [46]. For example, lower densities optimize cell growth, while higher densities optimize handling. A composite scaffold with a bi-density distribution might better satisfy both requirements.

FGF-2 was selected since it is both angiogenic (i.e. stimulates growth of new blood vessels) and osteogenic (i.e., stimulates bone growth) [47]; angiogenesis is the antecedent to osteogenesis [44,48]. A gradient of FGF-2 was selected because, in nature, spatial concentration gradients of endogenous growth factors (i.e., made by the body) play critical roles in directing cell migration, proliferation, and differentiation [49,50]. For example, during normal wound healing, cells from the wound site and invading host cells lose their blood supply due to

the injury. These cells respond by producing angiogenic growth factors that diffuse out into the surrounding healthy tissue. Growth factor concentration gradients, emanating from the hypoxic cells (i.e., lacking oxygen), are thus formed to provide chemotactic directional cues as liquid-phase (soluble) molecules. These cues direct angiogenic cell migration from surrounding vascularized tissues into and proliferation within the wound in order to induce angiogenesis. Spatial cues have been mimicked, to some extent, by tissue engineering therapies that use controlled growth factor release technologies to deliver growth factors as liquid-phase molecules [51]. Problems with this delivery approach include: 1) relatively large, non-physiogical doses of growth factors are required for the gradients to persist; and 2) liquid-phase delivery does not permit specific control over gradient directionality or growth factor localization within the scaffold. Growth factors have been immobilized within engineered scaffolds to begin to address persistence and dosing issues [52,53], but spatial patterning has not been accomplished [52,53]. We reason that, similar to chemotaxis, a solid-phase (growth factors immobilized to the scaffold) gradient of a low-to-high concentration of an angiogenic growth factor would direct cell migration into the scaffold, thus maximizing the cell population in the scaffold and enhancing therapeutic potential. The direction of the gradient was chosen because CSD studies have reported a significant quantitative difference in osteogenic cell sources to healing bone, with the dura (i.e. the protective, highly vascularized sheath of tissue between the skull and brain) representing the predominate cell source [54–56].

BMP-2 is a powerful osteogenic factor that stimulates bone precursor cells to differentiate into mature bone cells [57], i.e., it is present in the final stages of bone wound healing. When BMP-2 is delivered as a therapeutic factor, early differentiation of cells prior to sufficient migration and proliferation could inhibit further tissue growth, and thus inhibit wound healing. Therefore, temporal control of BMP-2 delivery will be important; that is, we want the cells to first have access to FGF-2, and later to BMP-2. By localizing BMP-2 in denser portions of the scaffold, the cells will take longer to degrade those portions of the scaffold and access the BMP-2 as discussed above.

We emphasize that we are not trying to replicate nature since CSD biology does not lead to bone regeneration on its own. Rather, we seek to create biologically inspired designs that might amplify and accelerate wound healing sufficiently to boost the body's own natural healing processes and promote CSD regeneration.

2.2. Fabrication of fibrin-based scaffolds

Fibrin hydrogel is produced by polymerization/gelation of the monomer fibrinogen to fibrin in the presence of the activator thrombin [58]. To fabricate fibrin-based scaffolds, the SFF system we are developing is configured with four ink-jet print heads for independently depositing solutions (bio-inks) of fibrinogen, thrombin, and two growth factors (Fig. 2). The print heads are focused at the printed surface where local mixing and gelation of deposited fibrinogen (Fg) and thrombin (Tr) droplets occur. Fibrin gelation times range from seconds to minutes.

The growth factor bio-inks consist of growth factors pre-bound to fibrinogen (GF/Fg). The deposited concentrations of growth factors are modulated by controlling the ratio of the GF/Fg bio-inks to the Fg bio-ink. Direct or indirect binding to native extracellular matrix biomolecules occurs naturally for most growth factors, including FGF-2 and BMP-2 [41]. However, since binding interactions between the growth factors and fibrinogen binding site(s) typically require between 30–60 min to reach equilibria [59], we premix the growth factors with fibrinogen and wait several hours prior to printing to minimize post printing diffusion of the growth factors. Thus, upon printing and gelation, these growth factors remain bound to fibrin to establish a solid-phase printed pattern that will persist in physiologically relevant concentrations until host cells invade and degrade the scaffold.

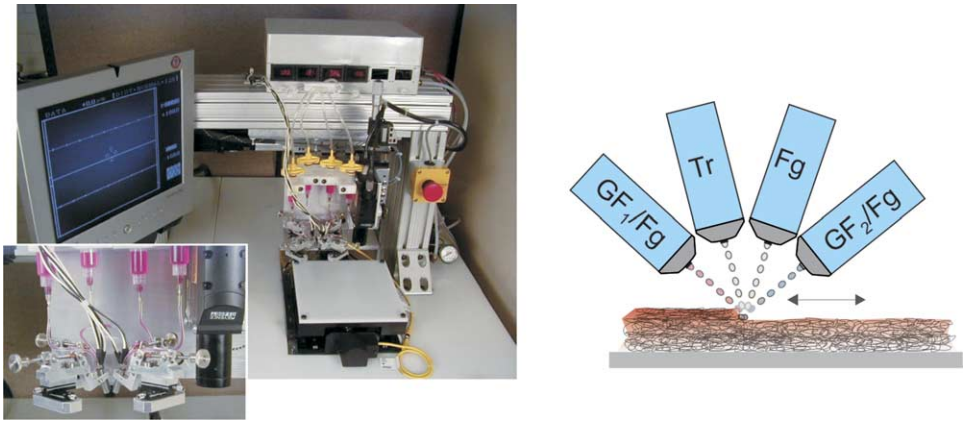

Fig. 2. SFF printing system configured with four ink-jet print heads for depositing fibrinogen (Fg), thrombin (Tr), and two growth factors (GF_1 and GF_2).

The ink jets are microsolenoid valves (Matthews International Corp., Pittsburgh, PA) with 100 μm diameter nozzles. The volume of jetted fluid, which is proportional to the valve open time and the supply pressure, can be controlled down to approximately 2 nl. The jets are mounted to computer controlled X-Y servo stages that move the jets relative to the substrate. A computer controlled Z-axis adjusts the substrate-to-print head stand-off height between layers using feedback from a confocal displacement sensor (Keyence Corp., Woodcliff Lake, NJ). The printer is enclosed within a filtered, laminar flow hood for sterility. The current system can produce features with a size resolution of 250 μm.

Examples of heterogeneous scaffolds printed with this system are shown in Fig. 3. Fig. 3a shows a scanning electron micrograph (SEM) of fibrin printed with 20 mg/ml of fibrinogen and 10 U/ml of thrombin. The resulting fibrin microstructure (fibril diameter and density) is similar to fibrin formed during bulk gelation [60,61]. Fig. 3b shows a concentration gradient of FGF-2 printed in a single layer of a 200 μm thick fibrin scaffold imaged for fluorescence using a binocular scope. The concentration of printed FGF-2 was modulated by controlling the ratio of two bio-inks: 100 μg/ml of cyanine 3 fluorescently-labeled FGF-2 (Cy3-FGF-2) pre-bound to 20 mg/ml of fibrinogen, and 20 mg/ml of fibrinogen alone. Fig. 3c shows a printed 3D cross-hatch pattern of variable density fibrin imaged as for Fig. 3b. The cross-hatch was produced by printing Cy3-fibrinogen with a bio-ink concentration of 12 mg/ml and the surrounding non-fluorescent cross-hatch fill was printed with 20 mg/ml unlabelled fibrinogen. The thrombin bio-ink concentration was 25 U/ml. This structure was printed with four 250 μm layers, creating an 8×8 mm square, 1 mm thick, bi-density structure. Fig. 3d is a schematic showing how the cross-hatch pattern was formed with interconnected regions of different fibrin densities.

3. Bayesian Modeling

Bayesian statistical inference is a collection of statistical methods for designing experimental studies and for analyzing data [62]. One begins with a statistical model that describes a relationship among the parameters that can be controlled (e.g., FGF-2 and BMP-2 concentrations and fibrin density) and the desired outcome (e.g., bone growth). The model involves unknown parameters to be estimated based on experimental data from in vivo experiments.

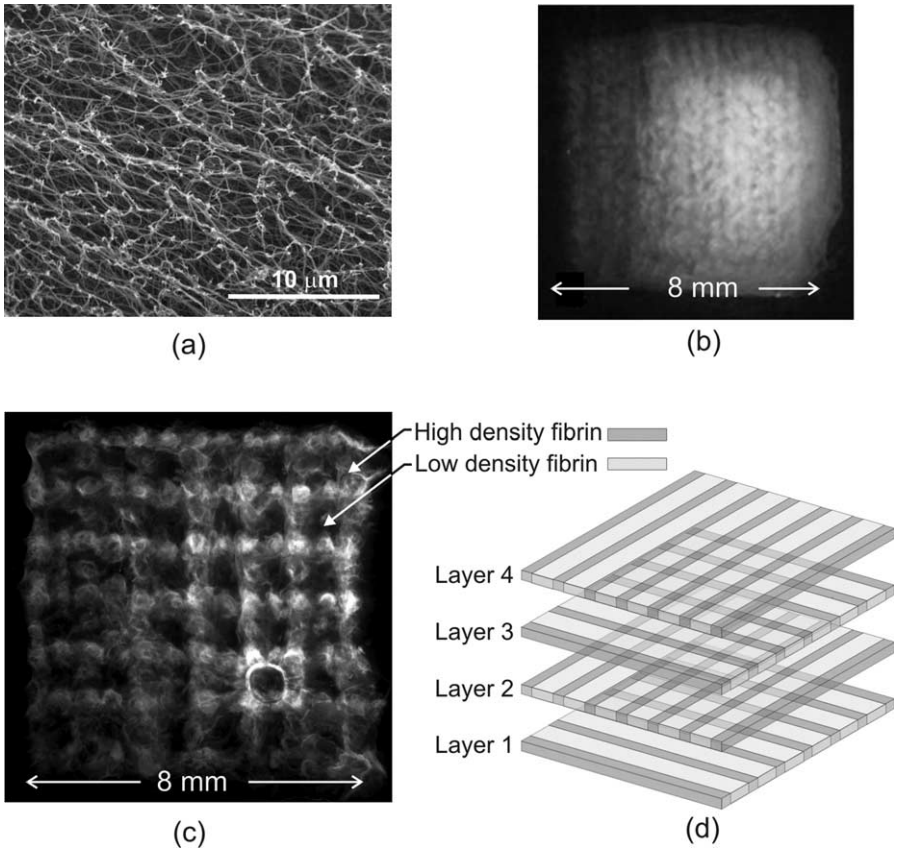

Fig. 3. (a). SEM of ink-jet printed fibrin. (b) Fluorescence image of a fluorescently labeled Cy3-FGF-2 concentration gradient printed in a 200 (μm thick fibrin scaffold layer. (c) 3D cross-hatch pattern of variable density fibrin printed using Cy3-fibrinogen printed with four individual 250 μm layers, creating a 1 mm thick, bi-porosity structure. (d) schematic of printing the layers to form a in interconnected, bi-density structure.

Bayesian statistical inference combines prior information expressed as a prior probability distribution for the parameters with available data to form a posterior probability distribution. Point estimates and confidence intervals can then be extracted from the posterior distribution.

In multi-stage Bayesian analysis, the statistical models are updated and improved sequentially through multiple stages of testing and data acquisition [35,63]. Using this multistage Bayesian approach, the results of each prior model and set of experiments guide the selection of the combination of experimental sample points for the next stage, thus reducing the required number of experiments and improving the quality of information obtained at each stage.

Bayesian methods are particularly useful in experimental design to estimate a response surface. A non-Bayesian method would observe a process on a grid of points and estimate the response surface based on the information gathered at those points, typically using a low order polynomial to model the response. Several improvements to this standard method can be implemented within the Bayesian framework. For example, a prior distribution can be placed on the response surface to express the idea that the surface is expected to be smooth. As experimental data are collected, the current posterior probability distribution is updated into a new posterior distribution. This posterior distribution can be used to locate new experimental sampling points that will lead to the highest expected information gain. Then the procedure is repeated in several stages. Even though smoothing and sequential design can be carried out in a non-Bayesian framework, the Bayesian approach provides a unified, efficient, and rigorous way to accomplish this.

Building Bayesian models in a multi-stage approach has several advantages. First, it gives adaptability to the data gathering process, allowing the use of already acquired information to influence the location of the sampling points for the next stage of data collection. In addition, building the surrogate in stages eases the computational burden of the calculations associated with the model, such as optimal sampling or maximum likelihood estimation of its parameters. Finally, the multi-stage development of these models resembles the experimental process in which knowledge is formulated, tested, and updated in stages of hypothesizing, experimentation, and critical analysis of the resulting data.

3.1. Mathematical formulation

MBSM is a technique of general applicability for the creation of surrogate models of the response of physical systems. In this methodology, the response of the system $Z(\vec{x})$ is considered to be governed by a known set of design parameters $\vec{x} = [x_1, \ldots, x_n]$. For example, in our specific application of computer-aided bone tissue engineering, the response of the system is a measure of bone growth, while the design parameters are the concentrations of FGF-2, BMP-2 and the fibrin densities of the fibrin/BMP-2 component of the scaffold.

Experiments performed with such a system, or with a computational model of it, yield the data set represented in Eq. (1):

$$D^{(s)} = \begin{bmatrix} x_{11} & x_{12} & \cdots & x_{1n} \\ \vdots & \vdots & & \vdots \\ x_{m1} & x_{m2} & \cdots & x_{mn} \end{bmatrix} \tag{1a}$$

$$Z_{D^{(s)}} = [\, Z(\vec{x}_1) \quad Z(\vec{x}_2) \quad \cdots \quad Z(\vec{x}_m)\,]^T \tag{1b}$$

where $D^{(s)}$ (size $m \times n$) is the design matrix, whose m rows correspond to different combinations of the design parameters $x_1, \ldots x_n$,, represented by the n columns of $D^{(s)}$. For each sampling point in the design matrix $D^{(s)}$, we obtain the response of the system, and this information is summarized in the $m \times 1$ response vector Z_D. All matrices are identified with a superscript stage index, (s), to indicate that the data collected from the experiments correspond to a specific stage in our multi-stage modeling process.

The observed responses of Eq. (1) are considered to be a partial realization of a Gaussian spatial random process $Z(\vec{x})$, which can be decomposed as the sum of a deterministic mean (trend) $M(\vec{x})$ and a zero-mean spatial random process $Y(\vec{x})$, with a given covariance structure, i.e.

$$Z(\vec{x}) = M(\vec{x}) + Y(\vec{x}) \tag{2}$$

with

$$E\big[Y(\vec{x})\big] = 0 \tag{3a}$$

$$\operatorname{cov}\big[Y(\vec{x}_i), Y(\vec{x}_j)\big] = c\Big(||\,\vec{x}_i - \vec{x}_j||;\ \vec{\theta}\Big) \tag{3b}$$

where $c\Big(||\vec{x}_i - \vec{x}_j||;\ \vec{\theta}\Big)$ is the covariance function of the random process and represents the covariance between the response variables at two different locations in the design space. This covariance is a parametric function of the distance between the observations; its parameters $\vec{\theta}$ are estimated based on the observed data via maximum likelihood. In the decomposition presented in Eqs. (2) and (3), the mean component $M(\vec{x})$ is a global approximation of the response while the random processes $Y(\vec{x})$ account for localized deviations from this mean, such that the surrogate model interpolates the response data.

Consistent with the stochastic model of Eq. (2), the best prediction of the responses of the system at any unsampled point $\vec{x}_0$ in the design space, at stage s, would be the expected value of the random process at that point, conditional on the observed data, *i.e.*

$$\vec{Z}_*^{(s)}(\vec{x}_0) = E\Big[\vec{Z}^{(s)} | D^{(s)}, Z_D\Big] \tag{4}$$

which can be interpreted as the mean of the spatial random process posterior to the data collection stage. With the assumption that the system responses are a realization of a Gaussian spatial random process, the conditional expectation of Eq. (4) becomes

$$Z_*^{(s)}(\vec{x}_0) = M^{(s)}(\vec{x}_0) + \left[\vec{C}^{(s)}(\vec{x}_0, D^{(s)})\right]^T \left[C_{D^{(s)}}^{(s)}\right]^{-1} \left[Z_D^{(s)} - M^{(s)}(D^{(s)})\right] \quad (5)$$

where $\vec{C}^{(s)}(\vec{x}_0, D^{(s)})$ is the covariance vector between the unsampled point and the samples of the current stage, $C_{D^{(s)}}^{(s)}$ is the covariance matrix of the samples, and $M^{(s)}(\cdot)$ is the (prior) mean. Typically, for the first stage of data collection and modeling, the mean component $M^{(s)}(\cdot)$ is modeled as a linear regression on the design parameters. On the other hand, in the multistage implementation of the methodology we set $M^{(s)}(\cdot)$ equal to the posterior expectation at the previous stage $Z_*^{(s-1)}(\bullet)$.

A more detailed mathematical description of the Bayesian computational methodology that provides the basis for our work is presented in Osio and Amon [35], and further developments, extensions and applications of the methodology can be found in the work of Leoni et al. [38,64], Pacheco et al. [37,63,65–67], and Romero et al. [68].

4. Example of Bayesian modeling applied to scaffold design

To illustrate how the Bayesian methodology can be applied to aid in the design of the scaffold illustrated in Fig. 1, we conduct simulated experiments using a hypothetical computer model of bone wound healing. The model relates the performance response (i.e. bone growth) to values of the therapeutic factors, and thus the model stands in for the true state of nature for the simulated experimental studies. Both Bayesian and factorial design methods are used to sample this space, but no a priori information about this model is incorporated in the sampling algorithms. We show that with a fixed number of experiments, the Bayesian approach best estimates the model of wound healing. Therefore, numerical optimization on the Bayesian-derived model would produce better estimates of optimal values to use in a final therapy design.

Since computational models of wound healing do not exist, we create a hypothetical model (Fig. 4) that obeys some simple rules about expected outcomes based upon our experience and the literature. We emphasize that this model is an over simplification of nature, but provides a relatively complex, non-trivial 3D performance surface to demonstrate our approach. The model obeys the following rules:

- Uni-modal, normal distributions for single growth factors: When a single therapeutic growth factor is delivered, the performance response will have a normal distribution. If the growth factor concentration is too low, then there is little effect. If the concentration is too high, there is a biological feedback mechanism which inhibits desired cell responses [69]. Furthermore, very high concentrations of powerful growth factors like BMP-2 can stimulate growth of undesirable cells such as tumor cells [70].
- Synergistic effect of multiple growth factors: growth factors can work synergistically [50], and therefore, the resulting performance of combined FGF-2 and BMP-2 will be better than for either individually.
- Bi-modal distribution for fibrin/BMP-2 density: as the fibrin density increases, the time constant for cellular access to the BMP-2 increases because it takes cells longer to degrade in this denser portion of the scaffold. Therefore, the performance begins to improve and reach a local maximum at a point where the temporal relationship between cellular access to BMP-2 and FGF-2 is optimal. A second local maximum is produced where the net amount of BMP-2, which increases with density of the fibrin/BMP-2 component, is at an optimal value as a single factor.

In this simplified model, bone growth is a function of three parameters: magnitude of the FGF-2 concentration gradient, BMP-2 concentration, and the fibrin density of the fibrin/BMP-2 component of the scaffold. In the plots, the three coordinates (x,y,z) represent these parameters, while

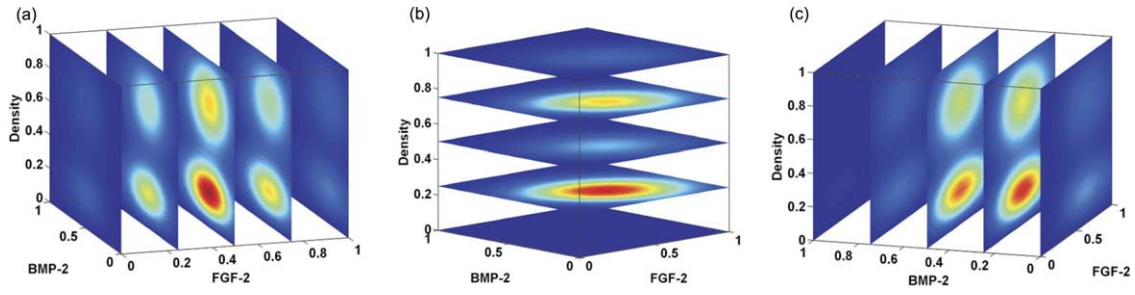

Fig. 4. Hypothetical model of bone growth in response to the therapeutic factors; magnitude of FGF-2 concentration gradient (FGF-2), BMP-2 concentration (BMP-2), and fibrin density in the fibrin/BMP-2 region of the scaffold (density).

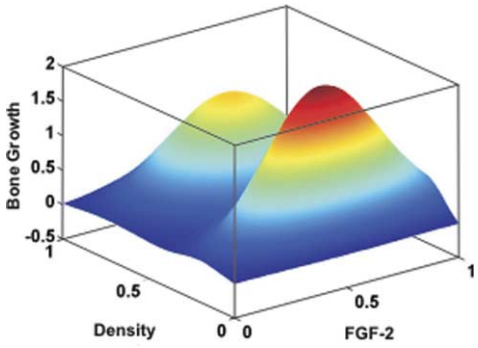

Fig. 5. Bone growth metric versus magnitude of FGf density of the fibrin/BMP-2 region for fixed BMP-2 = 25%.

the shaded colors represent the magnitude of resulting bone growth metric with red and blue indicating the zones of maximum and minimum bone growth, respectively. Each slice shown in the figures corresponds to a filled contour plot of the behavior of bone growth as a function of two of these parameters, while the third parameter is kept constant. For example, Fig. 4c shows the behavior of the bone growth metric as a function of the magnitude of the FGF-2 concentration gradient and fibrin density of the fibrin/BMP-2 region at five different values of BMP-2 concentration. Fig. 5 shows a 3D plot of the same data for BMP-2 concentration fixed at 25% of its range.

To illustrate MBSM, we simulate a set of experiments by sampling the hypothetical model in Fig. 4. The results of these experiments are used to construct a surrogate model of the system response and to select the combination of design parameters for the next stage of experimentation as discussed below.

For the first set of experiments, we construct a randomized orthogonal array of 25 sampling points, three variables, and strength two [71]. Orthogonal arrays have uniform projection properties that are desirable when exploring high-dimensional spaces. Fig. 6 shows the projection of this orthogonal array in planes formed by combinations of the design variables. Note that even though the orthogonal array is dispersed in the 3D space that we are exploring, it projects as a full factorial in each plane.

Once the first stage sampling points are selected, we simulate the experiments by evaluating the hypothetical bone growth model for each sampling point. With this data, we use maximum likelihood estimation to determine the model parameters that best fit the observed data, thus uniquely defining the first stage Bayesian surrogate model. Fig. 7 presents the resulting model for bone growth, using only 25 experimental points.

Based on the outcomes of the first set of experiments and the first stage Bayesian model as the prior probability distribution, we select a second set of 18 experimental design points using the optimal sampling strategy known as maximum entropy sampling [72]. The maximum entropy sampling strategy locates the sample points such that they maximize the expected information gain, thus reducing the uncertainty of the predicted response. Fig. 8 shows the projections of this experimental design in the planes defined by each pair of design variables. Fig. 8 also shows the first stage design for comparison purposes. Note that the distribution of points does not correspond to any

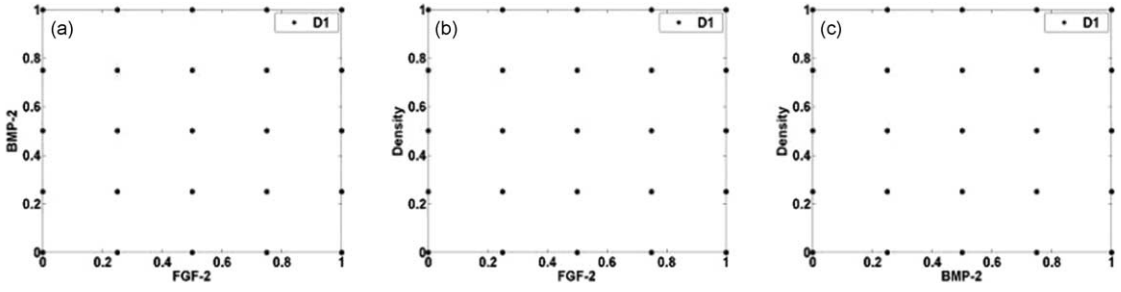

Fig. 6. Projections of the first stage experimental design, D1.

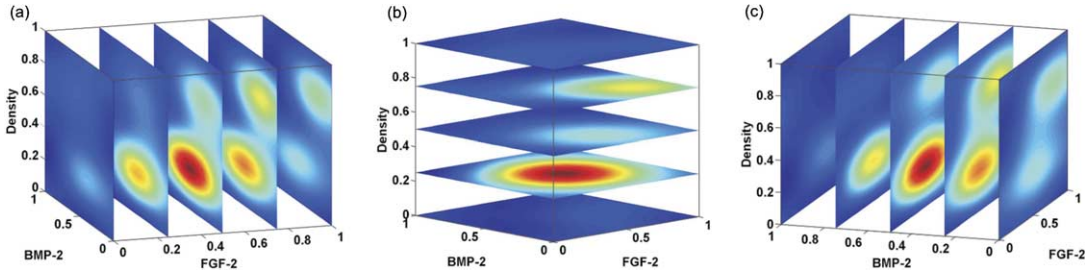

Fig. 7. First stage Bayesian surrogate model.

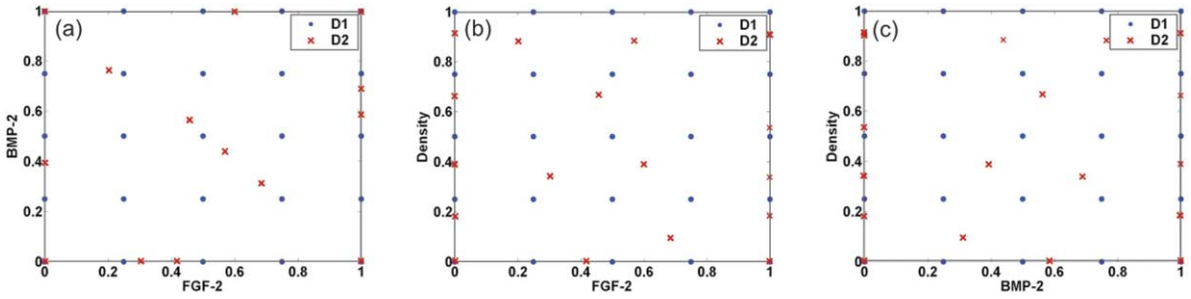

Fig. 8. Second stage Bayesian surrogate model.

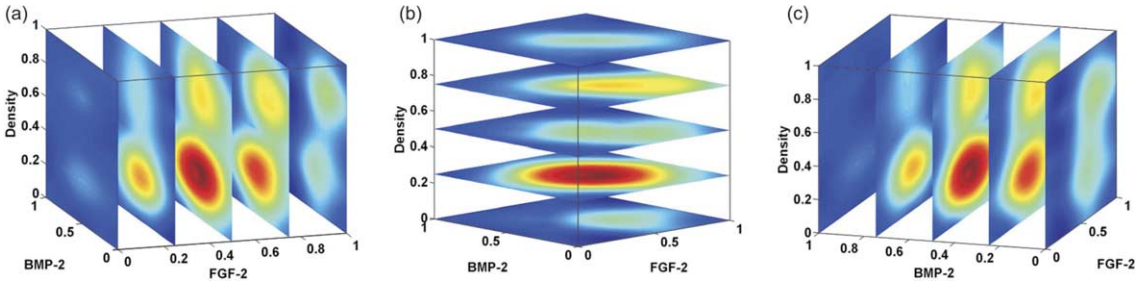

Fig. 9. Projections of the second stage experimental design D2.

standard experimental design, but rather it is tailored specifically for the phenomenon we are modeling. Note also that most of the points are located in the edges of the design space, mainly in regions that were left unsampled in the first stage of data collection. This behavior is to be expected from the maximum entropy sampling technique, since our knowledge of the response decreases as we move away from the regions of the space that have been sampled already.

After determining the experimental design for the second stage of data collection, we simulate the experiments by evaluating the hypothetical model at these points, and the observed responses are used to estimate the new model parameters via maximum likelihood. Fig. 9 shows the second stage surrogate model of the response; note the similarity with the true response shown in Fig. 4, even though the model is based on experimental data from only 43 samples. To evaluate the performance of the modeling methodology quantitatively, we calculate the mean relative error between the Bayesian surrogate model predictions and the hypothetical bone growth model used to generate the data. The resulting error after the second stage, averaged over an array of 100 points distributed uniformly in the design space, is only 6.73%, with a maximum error of 24.61%.

Next, we compare the MBSM methodology with the more traditional factorial approach for experimental design combined with low order polynomials to fit a response surface to the observed data points. Fig. 10 shows a full quadratic response surface model built based on a full factorial design of four values in three variables, with a total of 64 samples. For this case, the mean relative error is 8.00%, with a maximum error of 40.61%. Note that even though the response surface model was built with a larger number of samples (about 50% more samples were used), it results in larger prediction errors. The main reason for this

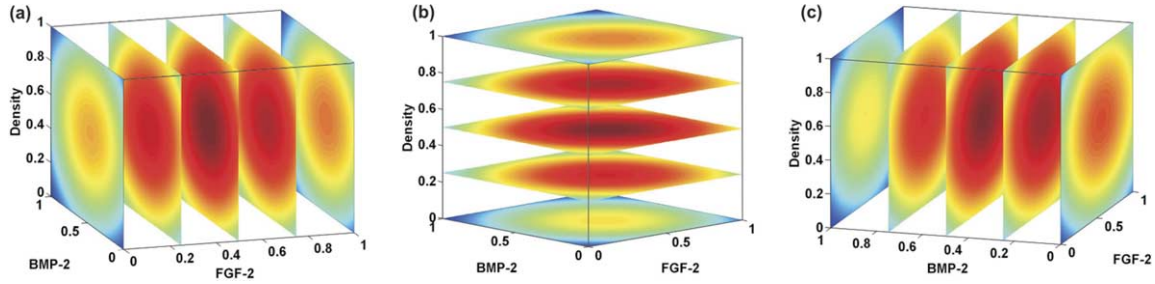

Fig. 10. Response surface model with linear, quadratic and interaction terms.

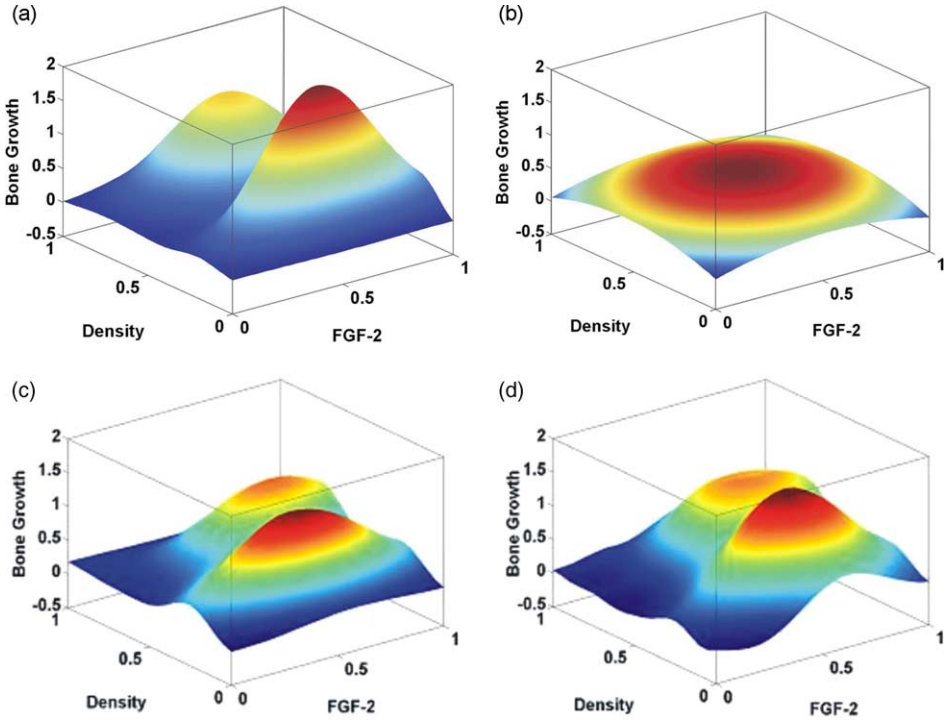

Fig. 11. Comparison of modeling methodologies. (a) Hypothetical model for bone growth. (b) Response surface model (64 samples). (c) First stage Bayesian surrogate model (25 samples). (d) Second stage Bayesian surrogate model (25 + 18 samples).

behavior is that response surface models are restricted to a given functional form, usually a second order polynomial on the input variables. As a result, the models lack flexibility to adapt to arbitrary shapes of the response over a large domain. In this application, the underlying model of bone growth is bi-modal, while the parametric form of the response surface constrains it to have only one maximum. Consequently, no matter how many samples are added to the response surface model, its performance will be poor. On the other hand, MBSM can adapt to response surfaces of arbitrary shape, and thus would yield smaller prediction errors as more samples are added to the model. Furthermore, due to the use of optimal sampling, multistage Bayesian models can give smaller prediction errors than response surface models while requiring a smaller number of samples, which can yield significant savings in experimental efforts and costs.

Fig. 11 summarizes our results, comparing the multi-stage Bayesian surrogate model to the response surface model with the hypothetical model of Fig. 4. To make visualization of the models easier, we fixed the concentration of BMP-2 at 25% of its allowed range. Fig. 11 shows surface plots of the bone growth metric as a function of the magnitude of the FGF-2 concentration gradient and fibrin density of the fibrin/BMP-2 component of the scaffold. Note the similarity between the surrogate models (Fig. 11c and d) with the hypothetical model for bone growth (Fig. 11a). Note also the improvement of the model from the first stage (Fig. 11c) to the second stage (Fig. 11d).

5. Conclusion

Biologically inspired scaffold designs for tissue engineering applications can be built with SFF processes such as the new fibrin-based printing system described in this paper. However, SFF also enables the space of design possibilities to expand dramatically, making it impractical to test experimentally all combinations of design parameter values using standard factorial analysis. To address this problem, we present a computer-aided, multi-stage Bayesian surrogate modeling approach that permits us to obtain more accurate models with fewer samples than would be required using factorial analysis. In addition to decreasing the number of samples required, models built using the Bayesian surrogate methodology can be expanded and refined over time. We showed how this methodology could be applied to heterogeneous scaffold designs. As an example, Bayesian versus traditional factorial design methods were compared to estimate response surface models for a simulated computer model of bone regeneration. The Bayesian method estimated the true surface within a mean relative prediction error of 6.73% and a maximum error of 24.61% compared with 8.00 and 40.61% for the factorial approach. Moreover, the

Bayesian-derived surface required only half as many experimental data points as the factorial approach to achieve these results. This capability will be particularly important for realizing next-generation scaffold designs and for shortening the timeline and reducing the expenses required to develop new therapies.

Acknowledgements

The authors gratefully acknowledge the funding of the Office of Naval Research (Grant no. N000140110766), the National Science Foundation (Grants no. CTS-0210238, CTS-0103082, and DMI-9800565), the National Institutes of Health (Grant no. 1 R01 EB00 364-01), the Pennsylvania Infrastructure Technology Alliance (PITA), a partnership of Carnegie Mellon, Lehigh University and the Commonwealth of Pennsylvania's Department of Community and Economic Development (DCED), the Health Resources and Services Administration (Grant no. 1C76 HF 00381-01), and the Scaife Foundation. We wish to thank Aventis Behring, L.L.C. (King of Prussia, PA) for their generous gift of lyophilized human fibrinogen and thrombin, and Matthews International Corp. (Pittsburgh, PA) for their generous donation of inkjet solenoid valves. We also acknowledge Dr Jeffrey Hollinger, Director of The Bone Tissue Engineering Center at Carnegie Mellon, for his insight on bone regeneration; Mr Larry Schultz and Dr Jason Smith for their assistance in the fabrication of matrices; and, Dr Greg Fisher for his assistance in imaging the scaffolds.

References

[1] Hollinger JO, Kleinschmidt JC. The critical size defect as an experimental model to test bone repair materials. J Craniofac Surg 1990;1:60–8.

[2] Schmitz JP, Hollinger JO. The critical size defect as an experimental model for craniomandibulofacial nonunions. Clin Ortho Rel Res 1986;205:299–308.

[3] Weiss L. Process overview, Analytical chapters NSF sponsored JTEC/WTEC panel report on rapid prototyping in Europe and Japan. International Technology Research Institute at Loyla College 1997;5–20.

[4] Kim SS, Utsunomiya H, Koski JA, Wu BM, Cima MJ, Sohn J, Mukai K, Griffith LG, Vacanti JP, et al. Survival and function of hepatocytes on a novel three-dimensional synthetic biodegradable polymer scaffold with an intrinsic network of channel. Ann Surg 1998;228:8–13.

[5] Levy RA, Chu TM, Halloran JW, Feinberg SE, Hollister S. CT-generated porous hydroxyapatite orbital floor prosthesis as a prototype bioimplant. AJNR Am J Neuroradiol 1997;18:1522–5.

[6] Wang F, Shor L, Darling A, Khalil S, Sun W, Guceri S, Lau A. Precision extruding deposition and characterization of cellular poly-e-caprolactone tissue scaffolds. In Solid freeform fabrication symposium, (Austin, Texas 2003;573–84.

[7] Kachurin AM, Stewart RL, Church KH, Warren WL, Fischer JP, Mikos AG, Kraeft S, Chen L, et al. Direct-write construction of tissue-engineered scaffolds. Mater Res Symp.: Materials Research Society; 2002.

[8] Das S, Hollister SJ, Flanagan C, Adewunmi A, Bark K, Chen C, Ramaswamy K, Rose D, Widjaja E, et al. Computational design, freeform fabrication and testing of nylon-6 tissue engineering scaffolds. In solid freeform fabrication symposium. Auting: University of Texas; 2002 p. 9–16.

[9] Cooke MN, Fisher JP, Dean D, Rimnac C, Mikos AG. Use of stereolithography to manufacture critical-sized 3D biodegradable scaffolds for bone ingrowth. J Biomed Mater Res 2003;64B: 65–9.

[10] Vozzi G, Previti MS, De Rossi D, Ahluwalia A. Microsyringe-based deposition of two-dimensional and three-dimensional polymer scaffolds with a well-defined geometry for application to tissue engineering. Tissue Eng 2003;8:1089–98.

[11] Cornejo I, McNulty TF, Lee S, Bianchi E, Tenhuisen K, Janas V, Danfroth S, Safari A, et al. Development of bioceramic tissue scaffolds via FDC. Ceramic Trans 2000;110:183–95.

[12] Zein I, Hutmacher DW, Tan KC, Teoh SH. Fused deposition modeling of novel scaffold architectures for tissue engineering applications. Biomaterials 2002;23:1169–85.

[13] Morissette SL, Lewis JA, Cesarano J, Dimos D, Baer T. Solid freeform fabrication of aqueous alumina-poly(vinyl alcohol) gel casting suspensions. J Am Ceram Soc 2000;83:2409–16.

[14] Lee G, Barlow JW. Selective laser sintering of bioceramic materials of implants. In solid freeform fabrication symposium. Austin: University of Texas; 1993 (p. 376–80).

[15] Lee G, Barlow J. Selective laser sintering of calcium phosphate powders. In Solid freeform fabrication symposium 1994 (The University of Texas at Austin), pp. 191–7.

[16] Leong KF, Phua KK, Chua CK, Du ZH, Teo KO. Fabrication of porous polymeric matrix drug delivery devices using the selective laser sintering technique. Proc Inst Mech Eng, [H] 2001;215: 191–201.

[17] Weiss L, Szem J. Assembled scaffolds for three dimensional cell culture and tissue regeneration. Patent no. 6,143,293. USA: Carnegie Mellon and University of Pittsburgh; 2000.

[18] Weiss L, Prinz F. Novel applications and implementations of shape deposition manufacturing.: Office of Naval Research; 1998. L(3).

[19] Weiss L, Merz R, Prinz F, Neplotnik G, Padmanabhan P, Schultz L, Ramaswami K, et al. Shape deposition manufacturing of heterogeneous structures. SME J Manuf Syst 1997;16:239–48.

[20] Weiss L. NSF workshop on design methodologies for solid freeform fabrication. Pittsburgh, PA: Carnegie Mellon University; 1995. NSF 96–216.

[21] Weiss L. Tissue engineering: solid freeform fabrication of scaffolds. Sci Med 2002;8:6–7.

[22] Cima M, Sachs E, Cima L, Yoo J, Khanuja S, Borland S, Wu B, Giordano R, et al. Computer-derived microstructures by 3D. Solid freeform fabrication symposium 1994 (The University of Texas at Austin), p. 181–190.

[23] Wilson Jr WC, Boland T. Cell and organ printing 1: protein and cell printers. Anat Rec 2003;272A:491–6.

[24] Mironov V, Boland T, Trusk T, Forgacs G, Markwald RR. Organ printing: computer-aided jet-based 3D tissue engineering. Trends Biotechnol 2003;21:157–61.

[25] Boland T, Mironov V, Gutowska A, Roth EA, Markwald RR. Cell and organ printing 2: fusion of cell aggregates in three-dimensional gels. Anat Rec 2003;272A:497–502.

[26] Ringeisen BR, Kim H, Young HD, Spargo BJ, Auyeung RCY. Cell-by-cell construction of living tissue. Mat Res Symp.: Materials Research Society; 2002.

[27] Marquez GJ, Renn MJ, Miller WD. Aerosol-based direct-write of biological materials for biomedical applications. Mat Res Soc Symp Proc.: Materials Research Society; 2002.

[28] Pitts J, Campagnola P, Epling G, Goodman S. Submicron multiphoton free-form fabrication of proteins and polymers: studies of reaction

efficiencies and applications in sustained release. Macromolecules 2000;33:1514–23.
[29] Klebe RJ. Cytoscribing: a method for micropositioning of cells and the construction of two- and three-dimensional synthetic tissues. Exp Cell Res 1988;179:362–73.
[30] Klebe RJ. Apparatus for the precise positioning of cells. Patent no. 5,108,926 1992.
[31] Sun W, Darling A, Starly B, Nam J. Computer aided tissue engineering, part I: overview, scope, challenges. J Biotechnol Appl Biochem 2004;39:29–47.
[32] Sun W, Starly B, Darling A, Gomez C. Computer aided tissue engineering, part II: application to biomimetic modeling and design of tissue scaffolds. J Biotechnol Appl Biochem 2004;39:49–58.
[33] Jin R, Chen W, Simpson TW. Comparative studies of metamodeling techniques under multiple modeling criteria. Struct multidisciplinary optimization 2001;23:1–13.
[34] Simpson TW, Peplinski JD, Koch PN, Allen JK. Metamodels for computer-based engineering design: survey and recommendations. Eng Comput 2001;17:129–50.
[35] Osio IG, Amon CH. An engineering design methodology with multistage Bayesian surrogates and optimal sampling. Res Eng Des 1996;8:189–206.
[36] Amon CH, Finger S. Combining experimental and statistical methods for quality improvement of microcasting in shape deposition manufacturing. Proceedings of the 1998 NSF design and manufacturing grantees conference. Mexico: Monterrey; 1998.
[37] Pacheco JE, Amon CH, Finger S. Flexible multistage Bayesian models for use in conceptual design. Fourteenth international ASME conference on design theory and methodology. Canada: Montreal; 2002.
[38] Leoni N, Amon CH. Bayesian surrogates for integrating numerical, analytical and experimental data: application to inverse heat transfer in wearable computers. IEEE transactions on components and packaging technol 2000;23:23–32.
[39] Doraiswamy S, Bayesian S. Bayesian analysis in engineering model assessment. ASME design engineering technical conferences. MD: Baltimore; 2000.
[40] Clarke HJ, Jinnah RH, Lennox D. Osteointegration of bone graft in porous-coated total hip arthroplasty. Clin Orthop Rel Res 1990;258: 160–7.
[41] Rifkin DB, Mazzieri R, Munger JS, Noguera I, Sung J. Proteolytic control of growth factor availability. Apmis 1999;107:80–5.
[42] Campbell PG, Wines K, Yanosick TB, Novak JF. Binding and activation of plasminogen on the surface of osteosarcoma cells. J Cell Physiol 1994;159:1–10.
[43] Wang JS. Basic fibroblast growth factor for stimulation of bone formation in osteoinductive or conductive implants. Acta Orthop Scand 1996;l269:1–33.
[44] Wang J, Aspenberg P. Basic fibroblast growth factor enhances bone-graft incorporation: dose and time dependence in rats. J Orthop Res 1996;34:316–23.
[45] Winn SR, Schmitt JM, Buck D, Hu Y, Grainger D, Hollinger JO. A tissue engineered bone biomimetic to regenerate calvarial critical-sized defects in athymic rats. J Biomed Mater Res 1999; 45:414–21.
[46] Bensaid W, Triffitt JT, Blanchat C, Oudina K, Sedel L, Petite H. A biodegradable fibrin scaffold for mesenchymal stem cell transplantation. Biomaterials 2003;24:2497–502.
[47] Bikfalvi A, Klein S, Pintucci G, Rifkin DB. Biological roles of fibroblast growth factor-2. Endocr Rev 1997;18:26–45.
[48] Wang JS, Aspenberg P. Basic fibroblast growth factor infused at different times during bone graft incorporation. Titanium chamber study in rats. Acta. Orthop. Scand. 1996;67:229–36.
[49] Tabata T. Genetics of morphogen gradients. Nat Rev Genet 2001;2: 620–30.
[50] Einhorn TA. In: Brighton CT, Freidlaender GE, Lane JM, editors. Enhancement of fracture healing by molecular or physical means: an overview. Bone formation and repair. Rosemont, IL: AAOS; 1994.
[51] Saltzman WM, Olbreicht WL. Building drug delivery into tissue engineering. Nat Rev Drug Discovery 2002;1:177–86.
[52] Sakiyama SE, Schense JC, Hubbell JA. Incorporation of heparin-binding peptides into fibrin gels enhances neurite extension: an example of designer matrices in tissue engineering. FASEB J 1999; 13:2214–24.
[53] Richardson TP, Peters MC, Ennett AB, Mooney DJ. Polymeric system for dual growth factor delivery. Nat Biotechnol 2001;19: 1029–34.
[54] Bosch C, Melsen B, Vargervik K. Guided bone regeneration in calvarial bone defects using polytetrafluoroethylene membranes. Cleft Palate Craniofac J 1995;32:311–7.
[55] Wang J, Glimcher MJ. Characterization of matrix-induced osteogenesis in rat calvarial bone defects: origins of bone-forming cells. Calcif Tissue Int 1999;65:486–93.
[56] Clark RA. Fibrin wound healing. Ann N Y Acad Sci 2001;936: 355–67.
[57] Wozney JM. The potential role of bone morphogenetic proteins in periodontal reconstruction. J Periodontol 1995;66:506–10.
[58] Mosesson MW. The assembly and structure of the fibrin clot. Nouv Rev Fr Hematol 1992;34:11–16.
[59] Sahni A, Odrljin T, Francis CW. Binding of basic fibroblast growth factor to fibrinogen and fibrin. J Biol Chem 1998;273:7554–9.
[60] Jockenhoevel S, Zund G, Hoerstrup SP, Chalabi K, Sachweh JS, Demircan L, Messmer BJ, Turina M, et al. Fibrin gel – advantages of a new scaffold in cardiovascular tissue engineering. Eur J Cardiothorac Surg 2001;19:424–30.
[61] Herbert CB, Nagaswami C, Bittner GD, Hubbell JA, Weisel JW. Effects of fibrin micromorphology on neurite growth from dorsal root ganglia cultured in three-dimensional fibrin gels. J Biomed Mater Res 1998;40:551–9.
[62] Lindley DV. Bayesian statistics—a review. Philadelphia: SIAM ed.; 1972.
[63] Pacheco JE, Amon CH, Finger S, Pacheco JE, Amon C, Finger S. Bayesian surrogates applied to conceptual stages of the engineering design process. ASME J Mech Des 2003;125:664–72.
[64] Leoni N. Integrating information sources into global models: a surrogate methodology for product and process development Mechanical Engineering, PhD Thesis, Carnegie Mellon University, Pittsburgh, PA; 1999.
[65] Pacheco JE, Amon CH, Finger S. Developing Bayesian surrogates for use in preliminary design. ASME design engineering technical conference, theory and methodology 2001.
[66] Pacheco JE. A methodology for surrogate model building in the engineering design process. PhD Thesis, Department of Mechanical Engineering, Carnegie Mellon University, Pittsburgh, USA; 2003.
[67] Pacheco JE, Amon CH, Finger S. Incorporating information from replications into Bayesian surrogate models. ASME international design engineering technical conferences 2003.
[68] Romero D, Amon CH, Finger S, Verdinelli I. Multi-stage Bayesian surrogates for the design of time-dependent systems. ASME 2004 international design engineering technical conferences. Salt Lake City, USA: American Society of Mechanical Engineers (ASME); 2004.
[69] Battegay EJ, Raines EW, Seifert RA, Bowen-Pope DF, Ross R. TGF-beta induces bimodal proliferation of connective tissue cells via complex control of an autocrine PDGF loop. Cell 1990;63: 515–24.
[70] Poynton AR, Lane JM. Safety profile for the clinical use of bone morphogenetic proteins in the spine. Spine 2002;27(1):S40–S8.
[71] Owen AB. Orthogonal arrays for computer experiments, integration and visualization. Statistica Sinica 1992;2:439–52.
[72] Shewry MC, Wynn HP. Maximum entropy sampling. J Appl Stat 1987;14:165–70.

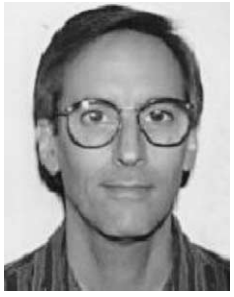

Lee Weiss is a Research Professor in the Robotics Institute of Carnegie Mellon University. He obtained his MSc in Bioengineering and PhD in Electrical and Computer Engineering from Carnegie Mellon. His current research interests include tissue engineering, computer-aided surgery, drug delivery using micro-electro-mechanical systems, and biological and chemical sensors.

Cristina Amon received her Engineering degree from Universidad Simon Bolivar and her MSc and ScD degrees from the Massachusetts Institute of Technology. She is the Raymond J. Lane Distinguished Professor of Mechanical Engineering, BioMedical Engineering and Director of the Institute for Complex Engineered Systems at Carnegie Mellon. She has been recognized with awards for research and education, including the ASEE George Westinghouse Award in 1997, SWE Distinguished Engineering Educator in 1999, ASME Gustus L. Larson Memorial Award in 2000, ASEE Ralph Coats Roe Award in 2002, and ASME Electronics and Photonics Packaging Division Award in 2004.

Susan Finger is on the faculty of the Civil and Environmental Engineering Department at Carnegie Mellon University. Dr Finger received a BA in Astronomy and an MA in Operations Research from the University of Pennsylvania. Her PhD is in Electric Power Systems through Civil Engineering from the Massachusetts Institute of Technology. She serves is a founder and Co-Editor-in-Chief of the journal Research in Engineering Design. Her research interests include representation languages for designs, integration of design and manufacturing concerns, and collaborative learning in design.

Eric Miller received his BS degree in Chemical Engineering from Carnegie Mellon University in 2002. He is currently in the third year of his PhD studies in the Biomedical Engineering Department at Carnegie Mellon University working on 2D and 3D growth factor patterning to direct cell organization.

David Romero is currently a PhD Candidate in Mechanical Engineering at Carnegie Mellon University, where he also obtained his MSc degree in Mechanical Engineering in 2003. David holds a Mechanical Engineer degree from the Universidad del Zulia, in Maracaibo, Venezuela, where he recently joined as an Assistant Professor in Mechanical Engineering. David's research interests are in the areas of engineering design, modeling and optimization, particularly in the thermal sciences.

Isabella Verdinelli is professor in residence at the Department of Statistics at Carnegie Mellon University. She is also professor of Statistics at the University of Rome. She did her undergraduate studies at the University of Rome, obtained a Master in Statistics from the University of London, and a PhD in Statistics from Carnegie Mellon University. Her current research interests include the statistical theory of multiple testing, Bayesian Experimental Design, and Statistical applications in Epidemiology, Clinical Trials, and Bioengineering.

Lynn Walker is an Associate Professor of Chemical Engineering at Carnegie Mellon University. She also holds courtesy appointments in the Departments of Chemistry and Materials Science and Engineering. She obtained her PhD from the University of Delaware. Her research interests include the rheology of complex fluids, controlling the nanostructure of soft materials and the quantifying the impact of fluid elasticity on interfacial flows.

Phil Campbell is a Research Associate Professor in the Institute for Complex Engineered Systems within CMU's Carnegie Institute of Technology. He received his PhD from Pennsylvania State University in 1988 in Physiology. His MS and BS were from Auburn University in 1981 and 1978, respectively, in Animal Sciences. Dr Campbell's specialty is endocrinology with his primary focus area in understanding hormone pericellular bioavailability as a basis for developing more effective hormone delivery therapies. His current research areas include applying these concepts to biological patterning using bio-printing techniques to better understand the underlying biological concepts of bone repair and regeneration.